

Photon number resolution using time-multiplexed single-photon detectors

M. J. Fitch,^{*} B. C. Jacobs,[†] T. B. Pittman,[‡] and J. D. Franson[§]
Johns Hopkins University, Applied Physics Laboratory, Laurel MD 20723-6099

Photon number-resolving detectors are needed for a variety of applications including linear-optics quantum computing. Here we describe the use of time-multiplexing techniques that allows ordinary single photon detectors, such as silicon avalanche photodiodes, to be used as photon number-resolving detectors. The ability of such a detector to correctly measure the number of photons for an incident number state is analyzed. The predicted results for an incident coherent state are found to be in good agreement with the results of a proof-of-principle experimental demonstration.

PACS numbers: 42.50.Ar, 85.60.Gz, 03.67.Hk, 07.60.Vg

I. INTRODUCTION

There has been considerable interest recently in the development of photon detectors that are capable of resolving the number n of photons present in an incident pulse. Photon number-resolving detectors of this kind are needed for a linear optics approach to quantum computing [1, 2], for example, and they may have other applications as well [3], such as conditional state preparation [4, 5]. Here we describe a simple time-multiplexing technique that allows ordinary single-photon detectors to be used as photon number-resolving detectors. The achievable performance of these devices is comparable to that of cryogenic devices [6, 7, 8] that are being developed specifically for number-resolving applications. Detectors based on an atomic vapor have also been proposed [9, 10].

Photon number-resolving detectors can be characterized in part by the probability $P(m|n)$ that m photons will be detected in a pulse that actually contains n photons. For linear optics quantum computing, it is essential that $P(n|n)$ be as close to unity as possible. As one might expect, this requires the single-photon detection efficiency η to be as large as possible in order to maximize the probability of detecting all of the photons present in a pulse. Silicon avalanche photodiodes (APDs) operating in the visible have a relatively large value of η and a small dark count rate, but they only produce a single output pulse regardless of the number of incident photons. The time-multiplexing technique described here avoids that limitation while retaining the large value of η and other potential advantages associated with the use of commercially-available APDs.

The basic idea of the time-multiplexing technique is to divide the incident pulse into N separate pulses of approximately equal amplitude that are displaced in time by a time interval Δt that is larger than the detector dead time τ . The probability that one of the divided pulses contains two or more photons becomes negligibly small

for $N \gg n$, in which case the fact that an APD can only produce a single output pulse is no longer a limitation.

Our implementation of such a time-multiplexed detector is illustrated in Figure 1. An incident pulse propagating in a single-mode optical fiber was divided equally into two paths using a 50/50 coupler. The difference L in path lengths was sufficiently large that the propagation times differed by more than the detector dead time. The two pulses were then recombined at a second 50/50 coupler and split equally into two more paths differing in length by $2L$, which results in four pulses all separated in time by Δt . This process was repeated once more with a path-length difference of $4L$, after which a fourth 50/50 coupler split the pulses again and directed them into one of two silicon APDs. The net result was the creation of $N = 16$ pulses of approximately equal amplitude. Unlike earlier approaches involving detector arrays [11, 12, 13, 14], this technique requires only two detectors, and it avoids the need for optical switches and a storage loop [15, 16, 17].

The remainder of this paper is organized as follows: In Section II, we present a theoretical analysis of the expected performance of a time-multiplexed detector (TMD) as a function of the detector efficiency and photon losses. The analysis makes clear that high detector

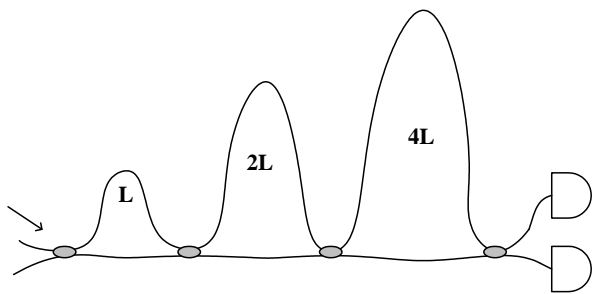


FIG. 1: Implementation of a time-multiplexed detector (TMD) for photon number-resolving applications. An incident pulse is divided into N weaker pulses separated by a time interval Δt using a series of fiber couplers and optical fiber delay lines. For sufficiently large values of N and Δt , this allows two ordinary silicon avalanche photodiodes to measure the number of incident photons with a probability of success that depends on their detection efficiency.

^{*}michael.fitch@jhuapl.edu

[†]bryan.jacobs@jhuapl.edu

[‡]todd.pittman@jhuapl.edu

[§]james.franson@jhuapl.edu

efficiency is needed for any photon number resolving detector, including the TMD and various cryogenic detectors under development [6, 7, 8]. Section III describes an experimental implementation of a TMD and the results obtained using coherent state inputs. A summary and conclusions are presented in Section IV.

II. THEORETICAL ANALYSIS

In the most likely application of a time-multiplexed detector, an incident pulse will contain an unknown number n of photons and the TMD is intended to measure the value of n . Since the measurement process destroys any coherence between states with different values of n , it is sufficient to consider an incident number state (Fock state) with a specific value of n and then calculate the response of the detector in the form of the probability distribution $P(m|n)$. The response to an incident coherent state will be considered in the next section.

It is therefore assumed that a number state $|n\rangle = (1/\sqrt{n!})(\hat{a}^\dagger)^n|0\rangle$ is incident on the initial 50/50 coupler, where the operator \hat{a}^\dagger creates a photon in the incident mode and $|0\rangle$ is the vacuum state. The effects of the first coupler can be described by the operator transformation

$$\hat{a}^\dagger \rightarrow (\hat{a}_s^\dagger + \hat{a}_l^\dagger)/\sqrt{2} \quad (1)$$

where the operators \hat{a}_s^\dagger and \hat{a}_l^\dagger create photons in the shorter and longer paths, respectively. Similar transforms can be applied to represent the remainder of the 50/50 couplers. After these transformations, the state vector will involve n photons distributed over 16 different modes.

It is important to include the effects of photon loss, which will degrade the performance of the device in a way that is similar to the effects of limited detector efficiency. The largest source of loss is absorption and scattering in the optical fiber. This can be described by the fraction f of the incident power that is transmitted through a length L of fiber. (In the experiments described in the next section, f has an approximate value of 0.97). The transmission through the fiber section of length $2L$ is then f^2 , etc. In order to simplify the analysis, it was assumed that the short sections of fiber have negligible length and that losses in the fiber connections are also negligible.

Losses in the optical fiber were included in the analysis by inserting an additional fiber coupler into each of the longer loops. The reflection and transmission coefficients of these couplers were adjusted to give a transmission probability of f (or the appropriate power of f) for each of the sections of fiber. An additional field mode corresponding to the photons removed from the loop by these couplers for each of the pulses was included in the state vector, which increased the total number of modes from 16 to 23. The effects of photon loss could then be taken

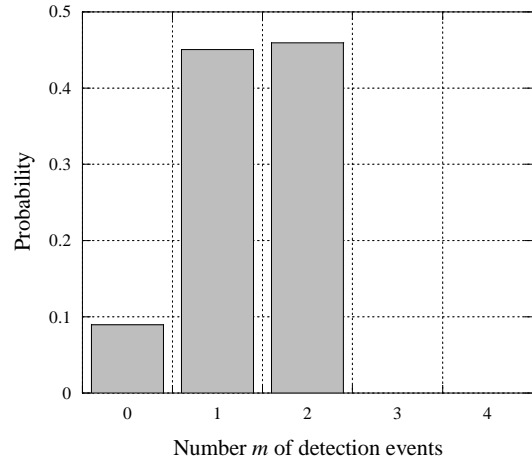


FIG. 2: The calculated probability distribution $P(m|n)$ for observing m detection events given that n photons were incident on a time-multiplexed detector. These results correspond to the case of two incident photons ($n = 2$) and a detector efficiency $\eta = 0.7$ with no loss ($f = 1$).

into account by applying operator transformations analogous to Eq. 1.

After all of the operator transformations had been applied, the state vector contained a large number of terms corresponding to all of the ways in which n photons can be distributed over the 23 modes. As a result, MATHEMATICA was used to sum the contribution of each term in the state vector to the probability distribution $P(m|n)$. In doing so, it was assumed that $P_0 = (1 - \eta)^q$, where P_0 is the probability that a detector will detect no photons if q photons are incident upon it. (This ignores any possible correlations between the effects of multiple photons.) The probability P_A that a detector will detect at least one photon and produce an output pulse is then given by $P_A = 1 - P_0$. Having determined the values of P_0 and P_A for each of the detectors, it was straightforward to calculate the probability of obtaining m detection events and add that contribution to the probability distribution $P(m|n)$ for each term in the state vector.

This analysis includes the fact that each of the 16 pulses will have different probabilities of reaching the detector, since they all travel through different lengths of optical fiber. In the limit of no loss ($f \rightarrow 1$) and perfect detection efficiency ($\eta \rightarrow 1$), the TMD is mathematically equivalent to a lossless multiport device, whose output properties can be obtained analytically [12]. Our numerical calculations agree with the analytic results in that limit.

Figure 2 shows the results of this analysis for the case of two incident photons ($n = 2$), which is a case of interest [1, 2, 18, 19, 20] in linear optics quantum computing. The detection efficiency was taken to be $\eta = 0.7$, which is typical of commercially-available silicon APDs, while the losses were assumed to be zero ($f = 1$) in this example.

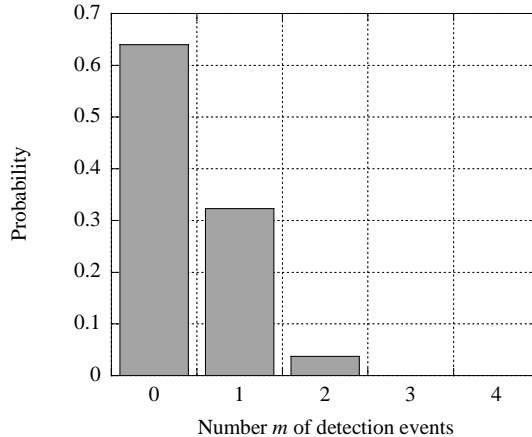


FIG. 3: Calculated probability distribution for observing m detection events when two photons are incident and the detection efficiency is 0.2 with no loss ($f = 1$), as in Fig. 2.

The limited value of $N = 16$ reduces the probability of detecting the correct number of photons to $15/16$, while the limited detection efficiency further reduces the probability of a successful measurement to $\sim 45\%$. It can be seen that a detection efficiency of 0.7 substantially limits the ability of a TMD to resolve the number of photons present in a pulse, even for the simple case of $n = 2$, and higher detection efficiencies will be required in order to improve the performance.

Similar results are shown in Figure 3 for the case of $\eta = 0.2$, which is comparable to the estimated external efficiency of the superconducting detector in Ref. [8]. Detectors of that kind are mathematically equivalent to taking the limit of large N , which would increase the probability of obtaining the correct photon number by 6% ($1/16$) above that shown in Figure 3. Nevertheless, it is apparent that further increases in the detection efficiency will be required.

Larger numbers of incident photons give a correspondingly smaller probability of measuring the correct value of n . As an example, Figure 4 shows the probability distribution $P(m|n)$ for the case of $n = 5$, $f = 0.97$, and $\eta = 0.43$. These parameters correspond to the experimental apparatus described in the next section, where the reduced value of η includes the combined averaged effects of input and output coupling loss, connector and splice losses, and excess losses in the fiber couplers.

More generally, the probability $P(n|n)$ of measuring the correct number of photons is plotted in Figure 5 as a function of the detector efficiency. For simplicity, the losses were assumed to be zero here, in which case $P(n|n)$ has the analytic result

$$P(n|n) = \frac{16!}{16^n(16-n)!} \eta^n \quad \text{for } n \leq 16 \quad (2)$$

as shown in the Appendix. In addition to the effects of

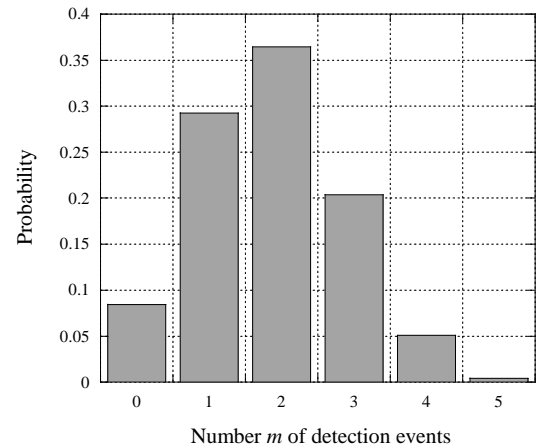


FIG. 4: Calculated probability distribution for m detection events for a Fock state with $n = 5$. Here the parameter values were $\eta = 0.43$ and $f = 0.97$ which correspond to the experimental conditions of Section III when the additional losses in the connections and couplers are included.

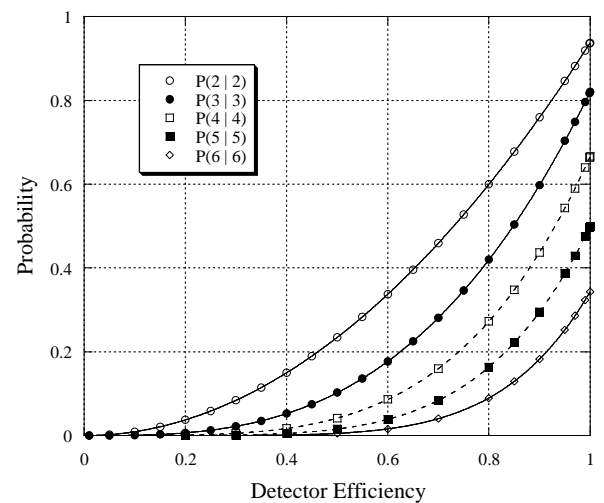


FIG. 5: Calculated probability $P(n|n)$ of detecting all n incident photons as a function of the effective detection efficiency η . The points were calculated numerically using the operator transformation technique of Eq. 1, while the lines correspond to the analytic formula of Eq. 2.

limited detector efficiency, it can be seen that the limited number of secondary pulses ($N = 16$) also has a significant effect as the value of n increases, even for perfect detector efficiency. At telecom wavelengths, the losses in optical fibers are much smaller and it should be possible to use much larger values of N .

III. EXPERIMENTAL RESULTS

In order to perform a proof-of-principle demonstration of a time-multiplexed detector, we implemented the TMD of Figure 1 using single-mode optical fiber and 2×2 fiber couplers designed to give 50/50 reflection and transmission at a wavelength of 702 nm. Since a source of number states is not currently available for large values of n , the experiments were performed using a weak coherent state. This was intended to allow a comparison of the theory with experiment and a demonstration of the basic feasibility of the TMD approach.

The input and output ports of the TMD had FC-style connectors while all of the other connections were made using a fusion splicer in order to minimize the losses. The two detectors were commercial silicon APD single-photon detectors (Perkin-Elmer model SPCM-AQR-13) with measured deadtimes of approximately 60 ns. The length L of the first long loop was chosen to be 22 m, which gave a delay between adjacent pulses of $\Delta t = 110$ ns, which was substantially larger than the deadtime. Short pulses (50 ps duration) were generated using an externally triggered fiber-coupled diode laser at 680 nm. A custom-made electronic circuit was used to count the total number of photon detections in a specified time window following each trigger. The triggering rate was kept sufficiently small that there was no overlap of the sequence of N pulses from two different triggering events.

The optical fiber used for the delay loops had a $4 \mu\text{m}$ core, which supported single-mode propagation of visible light (610 nm to 730 nm). The attenuation at 700 nm was specified by the manufacturer to be 6 dB/km, which corresponds to a transmission factor of $f = 0.97$. Small but significant losses also occurred in the input and output couplers, fusion splices, and excess loss in the 2×2 fiber couplers (typically 3% each). The total transmission of the fiber multiplexing device was measured to be 0.55, averaged over all N pulses.

The photon number distribution of the coherent state at one of the outputs of the TMD is given by a Poisson distribution:

$$P(\mu, n) = \frac{\mu^n e^{-\mu}}{n!} \quad (3)$$

where μ is the mean photon number. For a perfect detector ($\eta = 1$), $P(\mu, 0)$ would give the probability P_0 of detecting no photons. It can be shown from the linearity of the system that this result can be generalized to the case of an imperfect detector by replacing μ with $\mu' = \eta\mu$. (The limited detection efficiency is equivalent to placing an attenuator in front of the detector.) Thus $P_0 = \exp(-\mu')$ and $P_A = 1 - P_0$, where P_A is defined once again as the probability that a detector will detect at least one photon and produce an output pulse.

For values of f close to 1, the losses for all N pulses can be taken to be approximately the same without significantly affecting the distribution of the total number of

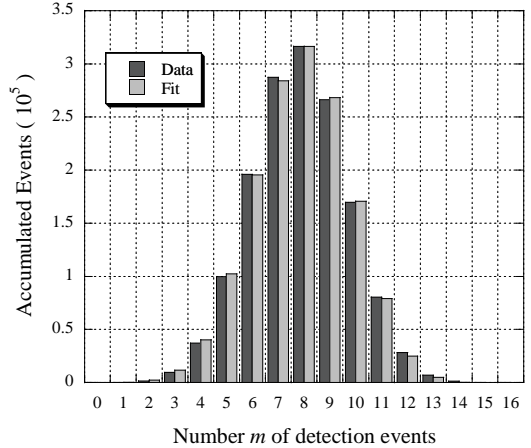


FIG. 6: Histogram of the number of events in which m photons were detected for an incident coherent state pulse with a relatively large intensity. The light bars correspond to the theoretical prediction of Eq. 4 based on a least-squares fit with $\eta l \mu_o = 13.1$, while the dark bars correspond to the experimental measurements.

counts. In that case, $\mu' = \eta l \mu_o / 16$ for each of the pulses incident on the detectors, where the transmission factor l accounts for the average total loss in the system (measured value $l = 0.55$), η is the APD detection efficiency (typ. 0.7), and μ_o is the mean number of photons incident upon the TMD. The probability $\mathcal{P}(m)$ of obtaining exactly m detection events (for $m \leq 16$) is then given by the binomial distribution

$$\mathcal{P}(m) = \frac{16!}{(16-m)!m!} (P_0)^{16-m} (1-P_0)^m. \quad (4)$$

A comparison of the theoretical predictions of Eq. 4 with the experimental results from a relatively intense coherent state are shown in Figure 6. The data corresponds to a histogram of the total number of events in which m photons were counted in an arbitrary data collection interval, which is proportional to the probability distribution $\mathcal{P}(m)$. The theoretical results correspond to a least-squares fit to Eq. 4 with two free parameters, a normalization constant (which reflects the length of the data collection interval) and the value of μ' , which corresponded to a best-fit value $\eta l \mu_o = 13.1$. It can be seen that the data are in relatively good agreement with the theoretical predictions. The small discrepancies between the theory and experiment are probably due to the approximation that all 16 pulses are subject to the same loss.

Similar comparisons of the theoretical predictions and the experimental results are shown in Figure 7 for a less intense coherent state ($\eta l \mu_o = 2.65$) and in Figure 8 for a relatively weak pulse ($\eta l \mu_o = 0.57$). It can be seen that a TMD can provide reliable estimates of the mean number of photons in a coherent-state pulse, but it can also be

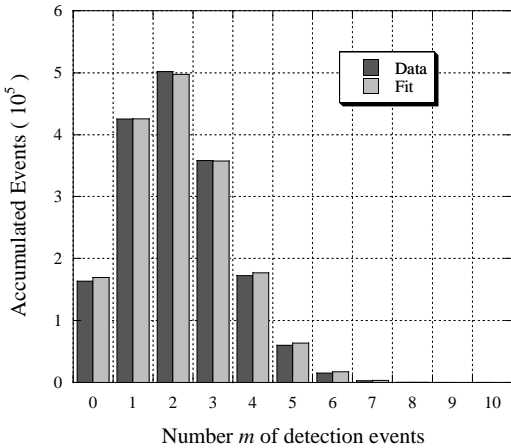


FIG. 7: Comparison of the theoretical prediction and experimental results for an incident coherent state with a smaller intensity than in Figure 6. Here the best fit corresponds to $\eta l \mu_o = 2.65$.

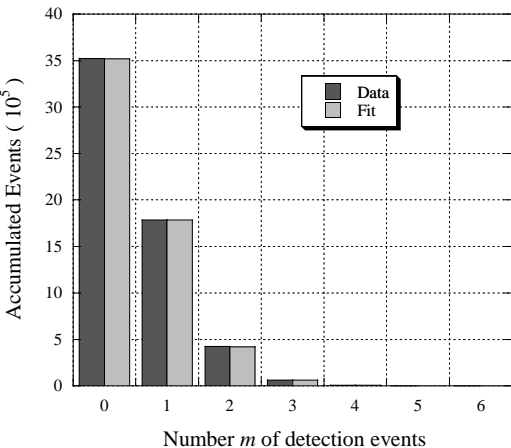


FIG. 8: Comparison of the theoretical prediction and experimental results for an incident weak coherent state input, as in Figure 6. Here the best fit corresponds to $\eta l \mu_o = 0.57$.

seen that the observed peak in the data is substantially less than the true mean number of photons.

IV. SUMMARY

In summary, we have described the use of time-multiplexing techniques to allow ordinary silicon avalanche photodiodes to be used as photon-number detectors. Although silicon APDs have high efficiencies and low dark counts, they only produce a single output pulse regardless of the number of photons that are incident. This difficulty can be avoided by splitting the incident pulse into a time sequence of N weaker pulses,

provided that $N \gg n$. The use of time multiplexing does lengthen the effective detector response time, which may also be of importance depending on the intended application [12, 21, 22, 23].

A proof-of-principle experiment was performed using optical fiber loops for the case of $N = 16$ and a coherent state input pulse. Good agreement was observed between the theoretical predictions and the experimental results.

The calculated response of a TMD to an incident number state makes it clear that high detection efficiencies will be required in order to truly resolve the number of photons in an incident pulse. But the same comment applies to any other detector intended for photon number-resolving applications, such as the cryogenic detectors that are being developed for that purpose. The results of our analysis suggest that the most important requirement for true number-resolving detectors is a high single-photon detection efficiency; an intrinsic ability to resolve photon numbers may be of lesser importance, since that capability can also be achieved using ordinary single-photon detectors.

Finally, we would like to note that a similar device has been independently demonstrated and analyzed by Achilles *et al.* [24].

APPENDIX:

In this Appendix, we provide a derivation of Eq. 2, and generalize it to arbitrary numbers of detected photons.

Non-classical photon statistics have been observed [25] at a multiport beam splitter when the path lengths are matched, and to describe such effects, a quantum formalism must be used (as in Section II above). In contrast, the path lengths in the TMD are far from matched, with relative delays of > 100 ns. As this is two or three orders of magnitude longer than the coherence length, the possibility of photon interferences can be neglected, and the relevant detection probabilities can be calculated from classical probability theory.

Let the input mode be evenly distributed to N output modes, so that a single photon on the input has a probability $1/N$ of reaching any given output mode. We further assume there are no losses, corresponding to $f = 1$ above, so this model describes a balanced, lossless N -port. At each output mode, there is a detector with efficiency η . Suppose that n photons are sent to the input. Let the probability of m detection events ($0 \leq m \leq n$) be written $P_\eta^N(m|n)$. In the case of zero detections, $P_\eta^N(0|n)$ is given by:

$$P_\eta^N(0|n) = (1 - \eta)^n \quad (\text{A.1})$$

which assumes that each photon fails to be detected with an independent probability of $1 - \eta$. For the case where all photons are detected, $P_\eta^N(n|n)$, must include a probability of $(\eta/N)^n$ for each of the ways in which a photon can be detected. Since all n photons must have gone to distinct output modes, there is a combinatoric factor

which counts the number of different ways to distribute n objects among N bins, so that:

$$P_\eta^N(n|n) = \left(\frac{\eta}{N}\right)^n \frac{N!}{(N-n)!} \quad \text{for } n \leq N. \quad (\text{A.2})$$

Eq. A.2 reduces to Eq. 2 for the special case in which $N = 16$.

For detectors of unit efficiency ($\eta = 1$), Paul *et al.* [12] gave a recursion relation for (in our notation) $P_{\eta=1}^N(m|n)$, along with a closed form solution. Their results can be extended to include non-unit detection efficiency by using the recursion relation:

$$\begin{aligned} P_\eta^N(m|n+1) &= P_\eta^N(m|n) \left[(1-\eta) + \frac{\eta m}{N} \right] \\ &\quad + P_\eta^N(m-1|n) \left[(N+1-m) \frac{\eta}{N} \right] \end{aligned} \quad (\text{A.3})$$

where the first term on the right hand side describes an additional photon failing to be detected or else exiting in a previously occupied output mode. The second term on the right hand side describes the detection of an additional photon in a previously unoccupied output mode. In the limit $\eta \rightarrow 1$, the recursion relation Eq. A.3 agrees with that given by Paul *et al.* (see Eq. 9 in Ref. [12]).

Using the boundary conditions of Equations A.1 and A.2, the recursion relation Eq. A.3 can be solved, with the result:

$$P_\eta^N(m|n) = \binom{N}{m} \sum_{j=0}^m (-1)^j \binom{m}{j} \left[(1-\eta) + \frac{(m-j)\eta}{N} \right]^n \quad (\text{A.4})$$

for $m \leq n \leq N$, where the binomial coefficient is $\binom{N}{m} \equiv N!/[m!(N-m)!]$. The derivation of Eq. A.4 is lengthy, but it can be verified that it satisfies the recursion relation.

Although Eqs. A.1 through A.4 were derived using classical probability theory, they give exactly the same numerical results as the field operator approach of Section II.

ACKNOWLEDGMENTS

We acknowledge useful discussions with M. T. Lamar. This work was supported by ARO, NSA, ARDA and IR&D funding.

[1] E. Knill, R. Laflamme, and G. J. Milburn, *Nature* (London) **409**, 46 (2001).
[2] J. D. Franson, M. M. Donegan, M. J. Fitch, B. C. Jacobs, and T. B. Pittman, *Phys. Rev. Lett.* **89**, 137901 (2002).
[3] A. Gilchrist, W. J. Munro, and A. G. White, *Phys. Rev. A* **67**, 040304R (2003).
[4] P. Kok, H. Lee, and J. P. Dowling, *The creation of large photon-number path entanglement conditioned on photodetection* (2001), quant-ph/0112002.
[5] H. Lee, P. Kok, N. J. Cerf, and J. P. Dowling, *Linear optics and projective measurements alone suffice to create large-photon-number path entanglement* (2001), quant-ph/0109080.
[6] J. Kim, S. Takeuchi, Y. Yamamoto, and H. H. Hogue, *Appl. Phys. Lett.* **74**, 902 (1999).
[7] S. Takeuchi, J. Kim, Y. Yamamoto, and H. H. Hogue, *Appl. Phys. Lett.* **74**, 1063 (1999).
[8] B. Cabrera, R. M. Clarke, P. Colling, A. J. Miller, S. Nam, and R. W. Romani, *Appl. Phys. Lett.* **73**, 735 (1998).
[9] A. Imamoğlu, *Phys. Rev. Lett.* **89**, 163602 (2002).
[10] D. V. F. James and P. G. Kwiat, *Phys. Rev. Lett.* **89**, 183601 (2002).
[11] S. Song, C. M. Caves, and B. Yurke, *Phys. Rev. A* **41**, 5261 (1990).
[12] H. Paul, P. Törmä, T. Kiss, and I. Jex, *Phys. Rev. Lett.* **76**, 2464 (1996).
[13] P. Kok and S. L. Braunstein, *Phys. Rev. A* **63**, 033812 (2001).
[14] P. Kok, *Limitations on building single-photon-resolution detection devices* (2003), quant-ph/0303102.
[15] K. Banaszek and I. A. Walmsley, *Optics Lett.* **28**, 52 (2003).
[16] J. Řeháček, Z. Hradil, O. Haderka, J. Peřina, and M. Hamar, *Multiple-photon resolving fiber-loop detector* (2003), quant-ph/0303032.
[17] O. Haderka, M. Hamar, and J. Peřina, *Experimental multi-photon-resolving detector using a single avalanche photodiode* (2003), quant-ph/0302154.
[18] T. B. Pittman, B. C. Jacobs, and J. D. Franson, *Phys. Rev. A* **64**, 062311 (2001).
[19] T. B. Pittman, B. C. Jacobs, and J. D. Franson, *Phys. Rev. Lett.* **88**, 257902 (2002).
[20] T. B. Pittman, M. J. Fitch, B. C. Jacobs, and J. D. Franson, *Experimental controlled-NOT logic gate for single photons* (2003), quant-ph/0303095.
[21] W. Schleich and J. A. Wheeler, *Nature* (London) **326**, 141 (1987).
[22] W. Schleich, D. F. Walls, and J. A. Wheeler, *Phys. Rev. A* **38**, 1177 (1988), and references therein.
[23] J. P. Dowling, W. P. Schleich, and J. A. Wheeler, *Annalen der Physik* (Leipzig) **48**, 423 (1991).
[24] D. Achilles, C. Silberhorn, C. Śliwa, K. Banaszek, and I. A. Walmsley, *Fiber-assisted detection with photon number resolution* (2003), submitted to *Opt. Lett.*, quant-ph/0305191.
[25] K. Mattle, M. Michler, H. Weinfurter, A. Zeilinger, and M. Zukowski, *Appl. Phys. B* **60**, S111 (1995).